Journal of Power Sources 184 (2008) 165–171

Contents lists available at ScienceDirect

Journal of Power Sources

journal homepage: www.elsevier.com/locate/jpowsour

Highly efficient single-layer gas diffusion layers for the proton exchange membrane fuel cell

T.F. Hung[a], J. Huang[b], H.J. Chuang[c], S.H. Bai[a], Y.J. Lai[a], Y.W. Chen-Yang[a,*]

[a] Department of Chemistry and Center for Nanotechnology, Chung Yuan Christian University, Chung-Li 32023, Taiwan, ROC
[b] Yeu Ming Tai Chemical Industrial Co., Ltd., Taichung 40768, Taiwan, ROC
[c] Materials and Electro-Optics Research Division, Electric Energy Section, Chung Shan Institute of Science and Technology, Lung-Tan 32544, Taiwan, ROC

ARTICLE INFO

Article history:
Received 25 March 2008
Received in revised form 25 May 2008
Accepted 26 May 2008
Available online 12 June 2008

Keywords:
Proton exchange membrane fuel cell
Single-layer gas diffusion layer
Carbon black
Poly(tetrafluoroethylene)
Vapor grown carbon nanofiber

ABSTRACT

In the present study, a series of highly efficient single-layer gas diffusion layers (SL-GDLs) was successfully prepared by the addition of a vapor grown carbon nanofiber (VGCF) in the carbon black/poly(tetrafluoroethylene) composite-based SL-GDL through a simple and inexpensive process. The scanning electron micrographs of the as-prepared VGCF-containing SL-GDLs (SL-GDL-CFs) showed that the GDLs had a microporous layer (MPL)-like structure, while the wire-like VGCFs were well dispersed and crossed among the carbon black particles in the SL-GDL matrix. Utilization of the SL-GDL-CFs for MEA fabrication was also done by direct coating with the catalyst layer. Due to the presence of VGCFs, the properties of the SL-GDL-CFs, including electronic resistivity, mechanical characteristic, gas permeability, and water repellency, varied with the VGCF content, with the overall effect beneficial to the performance of the proton exchange membrane fuel cell (PEMFC). The best performances obtained from the PEMFC with VGCFs at 15 wt.% was approximately 63% higher than those without VGCFs, and about 85% as efficient as ELAT GDL, a commercial dual-layer GDL, for both the H_2/O_2 and H_2/air systems.

1. Introduction

A promising alternative power plant for transportation, the proton exchange membrane fuel cell (PEMFC) boasts of high-energy efficiency, low emission, and low noise. This cell efficiency is determined by one of its core components: the membrane electrode assembly (MEA). Many factors, such as the amount of the catalyst [1–4], the type of proton exchange membrane [2,3,5], and the characteristics of the gas diffusion layer (GDL) [6–12], have been found to affect MEA efficiency. Among these factors, the GDL is a critical component for achieving high efficiency on the performance of PEMFC, with an ideal GDL requiring an optimal combination of the following: an effective path for the transport of gas reactants to the catalyst layers, a low electronic resistivity for the transmission of electrons, proper hydrophobicity for the prevention of water flooding, and a flexible surface for better contact with neighboring components. Recently, the effect of GDL's electronic resistivity on cell performance has been scrutinized through experimental investigations [9] and modeling studies [13,14]. The former revealed that while all other characteristics remained constant, the current density of the PEMFC increased with GDL's decreasing electronic resistivity [9]. As for modeling studies, these indicated that the lateral electronic resistivity of GDL, affected by the electronic conductivity, GDL thickness, and gas channel width, played a critical role in determining the current distribution and cell performance [13,14]. These results thereby confirmed the importance of reducing GDL's electronic resistivity for cell performance.

Our previous study prepared a novel single-layer gas diffusion layer (SL-GDL) based on the PTFE/carbon black composite [15]. Unlike the traditional multilayer GDL, the process for the preparation of the SL-GDL was simpler and less expensive. In addition, the as-prepared SL-GDL exhibited good mechanical property, high oxygen and air permeability, as well as sufficient water repellency, and it could be used without extra wet-proofing treatment and microporous layer (MPL) coating for MEA fabrication. Noteworthy too is that in both the H_2/O_2 and H_2/air systems, PEMFCs cell efficiencies fabricated with SL-GDL, including the current and power densities, were about half of that of ELAT GDL, which is a commercial dual-layer GDL with wet-proofing treatment and MPL on a non-woven web. Other factors might also affect PEMFCs performance; nevertheless, the discrepancies were mainly ascribed to SL-GDL's higher electronic resistivity caused by the disconnections between the carbon black particles, which are in turn due to the presence of the non-conductive PTFE. Therefore, diminution of electronic resistivity is one of the methods to further improve SL-GDL's efficiency on cell performance.

* Corresponding author. Tel.: +886 3 265 3317; fax: +886 3 265 3399.
E-mail address: yuiwhei@cycu.edu.tw (Y.W. Chen-Yang).

0378-7753/$ – see front matter © 2008 Elsevier B.V. All rights reserved.
doi:10.1016/j.jpowsour.2008.05.086

On the other hand, it is known that the vapor grown carbon nanofiber (VGCF), a graphitized carbon fiber with high aspect ratio, has high electronic conductivity, excellent mechanical properties, and a tendency to form a special network-like morphology [16–18]. It is for that reason that this study prepared a series of VGCF-containing SL-GDLs (SL-GDL-CFs) similar to the simple and inexpensive method used in SL-GDL [15]. The effects of VGCF on SL-GDL-CF properties were likewise studied and compared to those of SL-GDL and ELAT GDL. Moreover, the cell performance of the PEMFCs fabricated with as-prepared SL-GDL-CFs through direct coating with the catalyst layer and without extra wet-proofing treatment and MPL coating as applied on a conventional gas diffusion medium was also studied.

2. Experimental details

2.1. Preparation of VGCF-containing single-layer gas diffusion layers (SL-GDL-CFs)

The SL-GDL-CF samples were composed of carbon black (Vulcan XC-72, Cabot Co.), colloidal PTFE dispersion (D1-E, Daikin industries Ltd.), and vapor grown carbon nanofiber (VGCF; T-004, Yonyu Applied Technology Material Co., Ltd., Taiwan). The average size of the VGCF was approximately 30–100 nm in diameter and 1–10 μm in length. Preparation of the SL-GDL-CFs followed the same method used for SL-GDL preparation [15]. First, the VGCFs were dispersed in an appropriate amount of ethyl alcohol by an ultrasonic processor (VCX 750, Sonics & Materials, Inc.) with a frequency of 20 kHz. Sequential addition of the remaining ingredients to the dispersion was subsequently done; this was well mixed by a mechanical stirrer. The mixture was later calendered at room temperature and heat compressed under a pressure of approximately 75 kg cm^{-2}. Afterwards, the mixture was heated at 130 °C for 2 h to remove the residual solvent and then cooled to room temperature, resulting in the SL-GDL-CFs. These as-prepared SL-GDL-CF samples were homogeneous black sheets of about 0.38 ± 0.02 mm in thickness. The abbreviations and the corresponding compositions of the SL-GDL-CFs are summarized in Table 1. For comparison, ELAT LT 1200-N, which is a wet-proofed, MPL-coated, and non-woven webbed dual-layer GDL, was obtained from E-TEK Div. of De Nora N.A., Inc.; this was used as received.

2.2. Characterization and measurements

The morphology of the SL-GDL-CFs was characterized by a field-emission scanning electron microscope (FESEM, JEOL JSM-6330F). The electronic resistivity was measured by a four-point probe method using the combined system of a current supplier (AUTOLAB PGST30, Eco Chemie) and a voltmeter (Keithley 196). The measured current density and voltage were then converted to the corresponding electronic resistivity (Ω cm) [19]. Meanwhile, the mechanical properties of the as-prepared GDLs were determined using a tensile tester (Q-test) equipped with a 500 N load cell and a computer interfaced for data collection. All samples were prepared according to ASTM D638.

Table 1
Abbreviations and corresponding compositions of the GDL samples

Sample	Carbon black (wt.%)	Colloidal PTFE dispersion (wt.%)[a]	VGCFs (wt.%)[b]
TFCB-3[c]	70	30	0
SL-GDL-CF0	80	20	0
SL-GDL-CF5	80	20	5
SL-GDL-CF10	80	20	10
SL-GDL-CF15	80	20	15

[a] Based on the weight of the solid content in the dispersion.
[b] Based on the percentage of carbon black.
[c] Sample prepared in Ref. [15].

Concerning the GDLs' internal contact angles to water, these were determined via a combination of the Washburn method and Owens–Wendt calculation as previously reported [20]. The GDL sample was held by a metal clamp which was attached to a microbalance (AND, GR-120), while a beaker containing the test liquid was placed on a platform and was raised by a screw-type motor until the microbalance detected the GDL sample's contact to the liquid surface. The mass of liquid absorbed by the sample was recorded as a function of time through the computer interfaced with the microbalance. Consequently, the GDLs' internal contact angles to water and surface tensions were calculated according to the equations, as was described [20]. Five extra pure grade test liquids (*n*-hexane, acetone, methanol, toluene and benzyl alcohol; all acquired from ACROS Organic Company) were further applied for the measurements. All the results were determined with standard deviations based on the measurements of three samples for each GDL.

The GDL samples' gas permeability was performed by a gas permeability analyzer, which was designed as previously reported [5]. In the experiment, the inlet gas was humidified at 90 °C through a stainless steel water bottle, with the test temperature and flow rate of the inlet-humidified gas kept constant. The gas permeability coefficient (*P*, with unit of cm^3 (STP) cm/s cm^2 cm-Hg, also known as gas permeability) refers to the amount of gas, by volume, which penetrates a unit thickness and an area of specimen per unit time, under a constant temperature and unit pressure difference when the permeation is stable [21].

2.3. Fabrication of MEA and cell performance test

The as-prepared SL-GDL-CFs and the wet-proofed and MPL-coated ELAT GDL were separately coated with the catalyst layer to prepare the MEAs for use in the cell test. In preparation of the catalyst layer, 20 wt.% of Pt/C (HiSpec 3000, Johnson Matthey) was dispersed into 5 wt.% of Nafion solution (DE-2020, DuPont), keeping the weight ratio of Pt/C to the solid content of Nafion in the solution at 2 in order to form the slurry. The Pt/C slurry was then coated on the GDL sample by the spraying method. The amounts of Pt used were 0.3 mg cm^{-2} for the anode and 0.6 mg cm^{-2} for the cathode. The electrolyte membrane used was a Nafion membrane purchased from DuPont Company (NRE 212); this was pretreated according to a well-known membrane cleaning procedure prior to use [22], and was sandwiched between the two catalyst-coated GDLs at 140 °C under 70–75 kg cm^{-2} for 2 min. This resulted in a MEA of 25 cm^2 for a single cell test.

The corresponding single cell fixture was composed of the aforementioned MEA and a pair of graphite plates with a serpentine flow channel of 1 mm width and 1 mm depth. To circumvent the GDL from getting into the channels, the MEA (0.76 ± 0.04 mm in thickness) was placed between a pair of PTFE gaskets (TFE-15-25SP, Electrochem, Inc.), each of which has a thickness of 0.4 mm. Next, it was clamped between two stainless end plates, with eight bolts tightened to a uniform torque of 2.94 N m in order to ensure the GDLs' close contact with the graphite plates without getting into the channels.

During the test operation, the single cell fixture was connected to an in-house fuel cell test station. The fuel of the anode was hydrogen, and that of the cathode was either oxygen or air. Before cell testing, the leak test was performed with nitrogen gas to ensure that the single cell was gastight. Later, this single cell was operated at a constant voltage to activate the MEA until a stable current density was obtained [23]. The cell testing was carried out in both

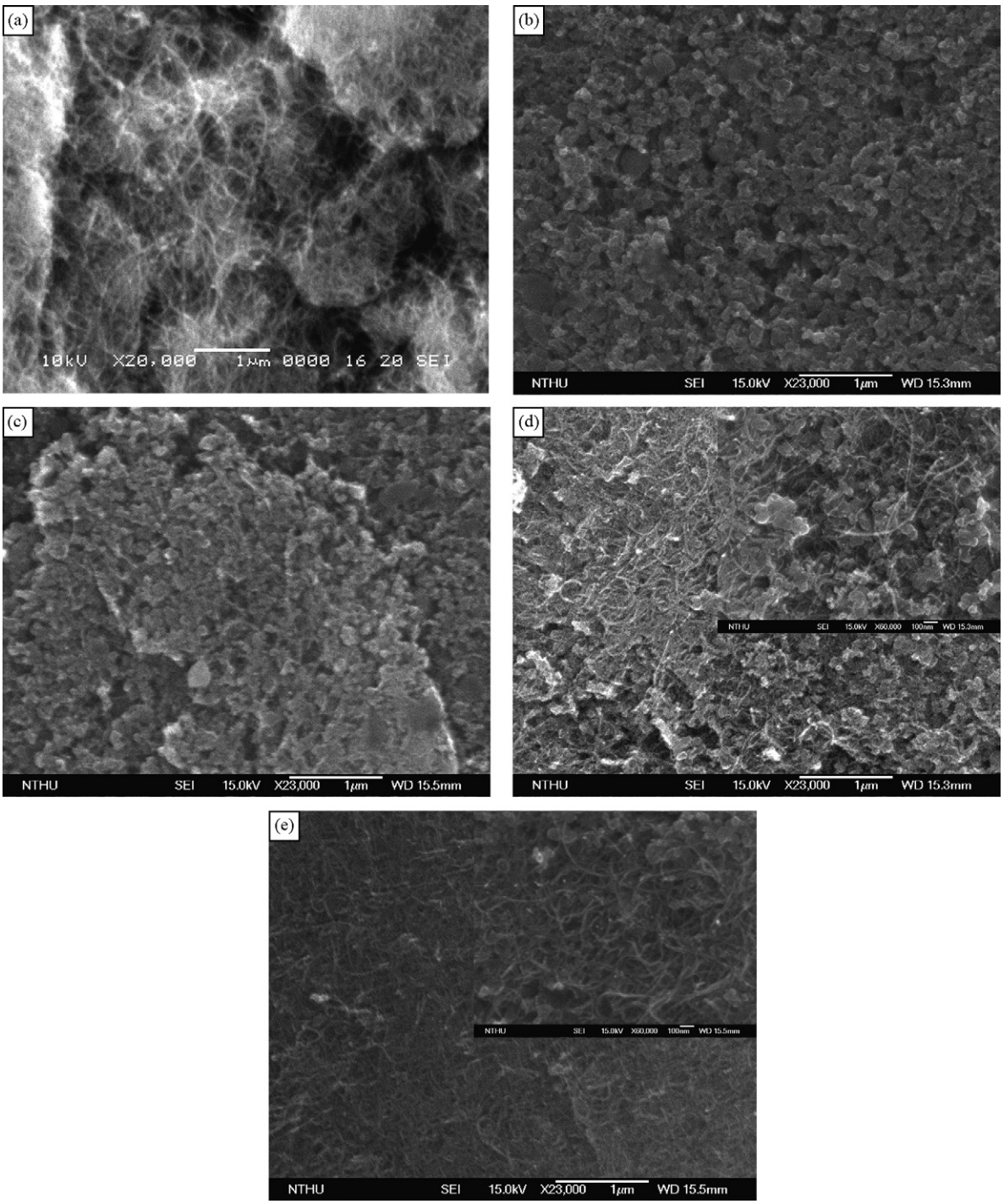

Fig. 1. SEM micrographs of the top-view of (a) pristine VGCFs and SL-GDL-CFx (b) $x = 0$, (c) $x = 5$, (d) $x = 10$ and (e) $x = 15$.

H_2/O_2 and H_2/air systems. For the H_2/O_2 system, the flow rates of the anode and cathode were 350 and 510 mL min^{-1}, respectively (corresponding to 1.6/2.3 of the stoichiometric ratio); for the H_2/air system, the flow rates of the anode and cathode were 350 and 710 mL min^{-1}, respectively (corresponding to 1.6/3.2 of the stoichiometric ratio). As for the operating temperatures of the anode humidifier, the cathode humidifier, and the cell, these were 80, 65, and 65 °C, respectively. The test was operated under an atmospheric pressure, and the cell efficiency was obtained both by controlling the cell voltage and by recording the corresponding stabilized current.

3. Results and discussion

3.1. Morphology of VGCF-containing single-layer gas diffusion layers (SL-GDL-CFs)

The SEM micrograph in Fig. 1 shows the top-view images of the pristine VGCFs and the as-prepared SL-GDL-CFs with various VGCF contents. Specifically in Fig. 1(a), the wire-like network morphology with high aspect ratio is observed for the pristine VGCFs [17], while Fig. 1(c–e) indicates that with the addition of VGCFs, all the SL-GDL-CFs remained in a MPL-like structure similar to the SL-GDL without

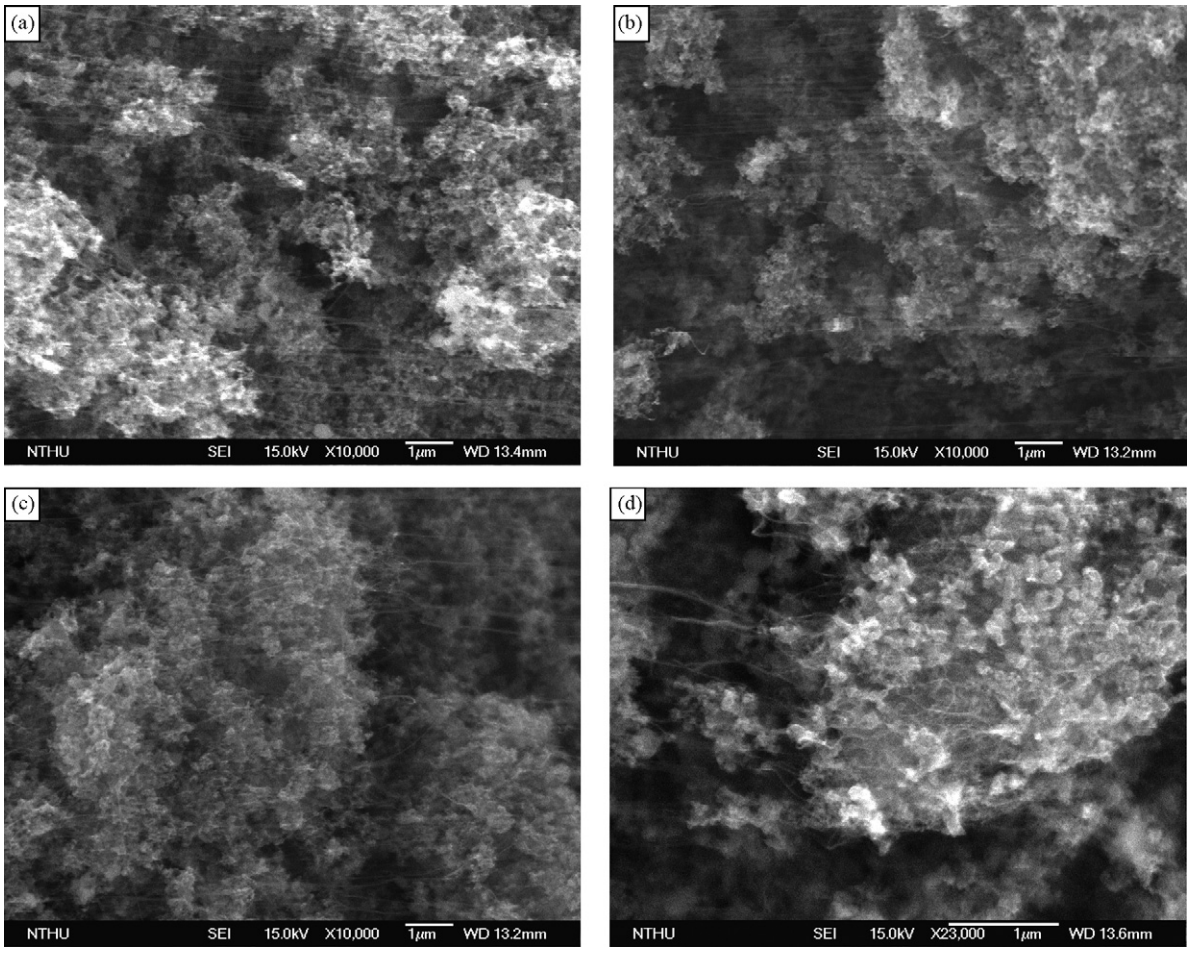

Fig. 2. SEM micrographs of the cross-section of SL-GDL-CFx: (a) $x = 0$, (b) $x = 5$, (c) $x = 10$ and (d) $x = 15$.

VGCF, as shown in Fig. 1(b); the latter figure likewise revealed that the SL-GDL-CF surfaces would be suitable for the catalyst coating in preparation of MEA as were the SL-GDLs. This also implies that basically, the presence of VGCFs did not significantly alter the surface morphology of SL-GDL. Furthermore, magnified micrographs as demonstrated in the inserts of Fig. 1(d and e) revealed satisfactory distribution of the wire-like VGCF networks among the carbon black particles, with interconnection of the particle surfaces and crossing of the pores formed by the three-dimensional arrangement of these carbon black particles. This is attributable to the good compatibility with carbon black by nature and the wire-like network morphology entangled among the carbon black matrix. The SEM micrographs of the SL-GDL-CF cross-sections shown in Fig. 2 further confirm the satisfactory distribution and interconnecting morphology of VGCFs in the carbon black matrix. The PTFE fibers bound on the carbon black particles and interconnected in the matrix were also found in SL-GDL-CF micrographs, similar to those observed in the SL-GDLs as previously reported [15], suggesting that a similar water-proof effect could be anticipated.

The above results indicate that unlike the conventional dual-layer GDL that is formed by a macroporous GDM layer and a microporous MPL layer [9], the prepared SL-GDL-CFs remained as a homogeneous single layer with the MPL-like structure similar to the prepared SL-GDL in the previous study. However, this is different from the corresponding SL-GDL and the conventional dual-layer GDL due to the presence of VGCF that subsequently alters its electronic resistivity, physical property, and reactant transport, thus influencing the performance of the corresponding PEMFC.

3.2. Electronic resistivity and physical properties of SL-GDL-CFs

The electronic resistivity of the SL-GDL-CF samples with various VGCF loadings, as well as that of the ELAT GDL, is presented in Table 2. As indicated, the electronic resistivity of SL-GDL-CF0 was about 47% less than that of TFCB-3 (from 0.540 Ω cm, this decreased to 0.285 Ω cm) due to 10 wt.% reduction of the non-conductive PTFE. Although less than 20 wt.% of PTFE loading could further decrease the electronic resistivity of SL-GDL, its water repellency, however, would be decreased [22,24], and the mechanical property would be accordingly reduced, making the material too brittle to form a useful GDL. As a result, the SL-GDL-CF samples were prepared with 20 wt.% of PTFE in this study.

It can also be observed in Table 2 that the electronic resistivity of SL-GDL-CF was decreased by another 28% (0.223 Ω cm) when 5 wt.% of VGFCs was added in the SL-GDL, and it further decreased with an increase of VGCF loading by up to 15 wt.%. The lowest value obtained from SL-GDL-CF15 was 0.187 Ω cm, which is 34% lower than that from SL-GDL-CF0. The decrement is ascribed to the formation of extra electron transport bridges provided by wire-like VGCFs interconnecting the disjoined carbon black particles. This was evidenced by the SEM micrographs and was previously discussed.

The mechanical properties of the SL-GDL-CFs, including yield stress and yield elongation, are also listed in Table 2. As indicated, when the solid content of the colloidal PTFE dispersion was decreased from 30 to 20 wt.%, the yield stress and yield elongation of SL-GDL-CF0 were accordingly decreased by about 55% and 63% from that of TFCB-3. This is attributable to the decrease of the

Table 2
Electronic resistivity and physical properties of the GDL samples

Sample	Electronic resistivity (Ω cm)	Yield stress (MPa)	Yield elongation (%)	Oxygen permeability $\times 10^2$ (cm^3 (STP) cm/s cm^2 cm-Hg)	Air permeability $\times 10^2$ (cm^3 (STP) cm/s cm^2 cm-Hg)
TFCB-3[a]	0.540	0.9	79	2.4	2.7
SL-GDL-CF0	0.285	0.4	29	4.5	4.9
SL-GDL-CF5	0.223	0.5	8	2.3	2.1
SL-GDL-CF10	0.209	0.5	9	2.0	1.8
SL-GDL-CF15	0.187	0.5	10	1.6	1.6
ELAT GDL[a]	0.020	1.0	0.9	0.9	0.5

[a] Results reported in Ref. [15].

PTFE fibers formed from the colloidal PTFE dispersion interconnecting the carbon black particles throughout the matrix. Moreover, it reveals that the mechanical properties of the as-prepared SL-GDLs were significantly dependent on the content of the colloidal PTFE dispersion. Likewise, with the addition of VGCFs, the yield stresses of all the SL-GDL-CFs increased to about 0.5 MPa, and the yield elongations reduced to the range of 8–10%, making them mechanically stronger than SL-GDL-CF0. This is due to the intrinsic reinforcement property of VGCFs entangled in the carbon black matrix as observed in the SEM images. On the other hand, the results indicate that all the as-prepared SL-GDL-CF samples had less yield stress but larger yield elongation than the non-woven webbed ELAT GDL, but they are strong enough for the MEA fabrication of PEMFC.

Meanwhile, the Washburn constants, internal contact angles to water (θ_{H_2O}) and the surface tensions of the GDL samples are shown in Table 3. It is found that as the content of the colloidal PTFE dispersion decreased from 30 to 20 wt.%, the θ_{H_2O} of SL-GDL-CF0 decreased by about 32% that of the TFCB-3. This is ascribed to the decrease of the hydrophobic PTFE fibers' content interconnected throughout the matrix. It is also of note that the θ_{H_2O} values were further decreased slightly with increased VGCF loading due to the reduction of PTFE's relative content.

3.3. Gas permeability of SL-GDL-CFs

The uniform and efficient transport of gas reactants from the electrodes to the catalyst surfaces is one of the vital functions required of an ideal GDL during PEMFC operation. It is well known that current is affected by the kinetics of the reaction at a low current density region; while by the diffusion of the reactants at a high current density region [6]. Consequently, an investigation of the GDL's gas permeability is important for studying the mass transport of a fuel cell. As demonstrated in Table 2, the gas permeabilities of SL-GDL-CF0 was about 88% and 82% higher than the values obtained from TFCB-3 for humidified oxygen and humidified air, respectively. This is attributable to the higher content of carbon black particles in the SL-GDL, thereby constructing more gas flow channels for the gas transport. However, the SL-GDL-CFs' gas permeabilities decreased with the increased VGCF loading for both humidified oxygen and humidified air. This may be, for the most part, due to the change of the solubility of humidified gas with the reduction of the hydrophobic PTFE's relative content. Nevertheless, all the SL-GDL-CF samples showed higher gas permeabilities than ELAT GDL for both humidified gases as SL-GDL-CF samples are single layered and provided uniform gas flow channels; in contrast, ELAT GDL is a dual-layered sample and contained both a macroporous gas diffusion medium (GDM) and a MPL, which then hindered gas transport at the interface [9].

The results discussed above show that the prepared SL-GDL-CFs in this study have adequate hydrophobic property and MPL-like surface structure; consequently, they can be used as GDLs for the fabrication of MEA through direct coating with the catalyst layer. This signifies that the process of preparation of the SL-GDL-CF has fewer steps and results in lesser cost than that of the traditional GDL.

3.4. Cell performance of PEMFC test

To evaluate the efficiency of the as-prepared SL-GDL-CFs on PEMFC performance, the MEAs of the PEMFCs were fabricated with the Nafion membrane (NRE 212) and the catalyst layer-coated SL-GDL-CFs with various VGCF loadings. The polarization curves of the as-prepared PEMFCs measured in the H_2/O_2 and H_2/air systems are plotted in Figs. 3 and 4. As illustrated, the open circuit potentials (OCP) of the as-prepared PEMFCs were in the range of 0.94–0.96 V

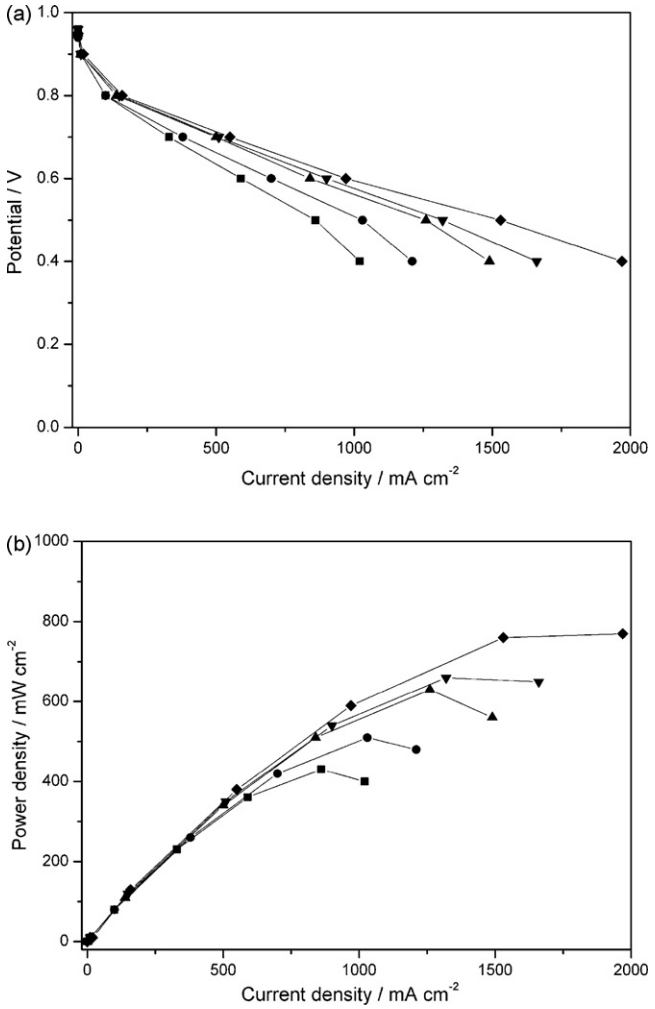

Fig. 3. Polarization curves of PEMFC with SL-GDL-CFx and ELAT GDL in the H_2/O_2 system: (a) *I–V* and (b) *I–P* curves (■) *x* = 0, (●) *x* = 5, (▲) *x* = 10, (▼) *x* = 15, (♦) ELAT GDL.

Table 3
Washburn constant, internal contact angles and surface tensions of the GDL samples

Sample	Washburn constant ($\times 10^6$ cm^5)	θ_{H_2O} (deg.)	γ_{SV}^{d} [a] (mN m^{-1})	γ_{SV}^{p} [b] (mN m^{-1})	γ_{SV} [c] (mN m^{-1})
TFCB-3[d]	1.70 ± 0.02	92 ± 7	8 ± 5	11 ± 8	19 ± 2
SL-GDL-CF0	1.38 ± 0.01	63 ± 4	5 ± 1	39 ± 4	44 ± 3
SL-GDL-CF5	1.27 ± 0.01	61 ± 5	6 ± 2	37 ± 3	43 ± 2
SL-GDL-CF10	1.46 ± 0.03	58 ± 5	4 ± 1	41 ± 3	45 ± 2
SL-GDL-CF15	1.45 ± 0.03	57 ± 7	5 ± 2	40 ± 2	45 ± 1
ELAT GDL[d]	1.58 ± 0.02	79 ± 2	4 ± 2	23 ± 6	27 ± 4

[a] Dispersive component of surface tension of solid–vapor interface.
[b] Polar component of surface tension of solid–vapor interface.
[c] Surface tension of solid–vapor interface.
[d] Results reported in Ref. [15].

for the H_2/O_2 system and 0.91–0.93 V for the H_2/air system. These results were as high as the values reported for the PEMFC with the traditional wet-proofed and MPL-coated GDLs [2,5–9], as well as that of the SL-GDLs reported in our previous study [15]. This is due to the characteristic single layer of SL-GDL-CFs in which fuels were delivered directly from the GDLs to the catalyst layers.

Additionally, it was also found that the cell performances measured in both testing systems increased with the increasing VGCF loading. In the H_2/O_2 system, the best current density of the PEMFC with SL-GDL-CF15 at 0.4 V was 1660 mA cm^{-2}, with its power density at 650 mW cm^{-2}. These values were approximately 63% higher than that with SL-GDL-CF0. On the other hand, the current and power densities at 0.4 V in the H_2/air system were 640 mA cm^{-2} and 250 mW cm^{-2}, respectively; this was about 25% higher than the values obtained from the PEMFC with SL-GDL-CF0. It was also noted that in both H_2/O_2 and H_2/air systems, the cell efficiencies of the PEMFC with SL-GDL-CF15 reached approximately 85% that of the ELAT GDL, that is, the SL-GDL-CF15 was approximately 85% as efficient as ELAT GDL on the PEMFC performance in both systems.

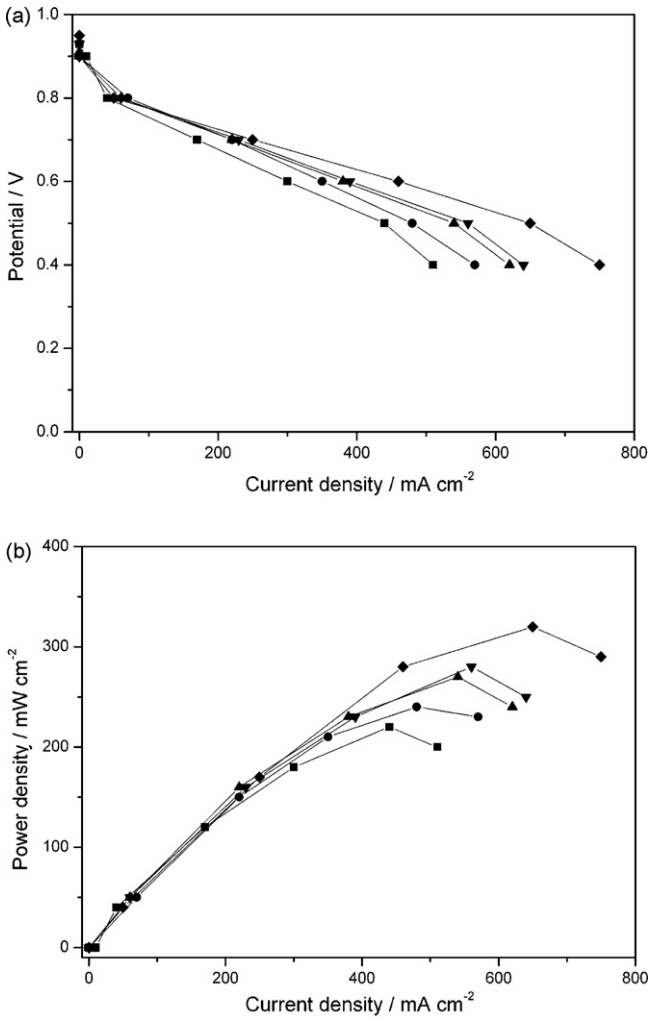

Fig. 4. Polarization curves of PEMFC with SL-GDL-CFx and ELAT GDL in the H_2/air system: (a) *I–V* and (b) *I–P* curves, (■) *x* = 0, (●) *x* = 5, (▲) *x* = 10, (▼) *x* = 15, (♦) ELAT GDL.

In summary, with the addition of wire-like VGCFs into the SL-GDL matrix, not only the electronic resistivity but also the related properties (water-repellency, mechanical property and gas permeability) of SL-GDL were influenced. The overall effect was beneficial to the performance enhancement of PEMFCs in both H_2/O_2 and H_2/air systems.

4. Conclusions

Highly efficient single-layer gas diffusion layers, based on carbon black and colloidal poly(tetrafluoroethylene) dispersion and designed for PEMFC, were successfully prepared in this study by the addition of VGCF through a simple and inexpensive process. The SEM micrographs indicated that the wire-like VGCFs were well dispersed in the SL-GDL matrix, and the VGCF-containing SL-GDLs (SL-GDL-CFs) were in MPL-like structure. The related properties of SL-GDL-CFs, including electronic resistivity, mechanical properties, contact angle to water, and gas permeability, varied with VGCF loading. It was also found that the existence of VGCFs is beneficial in reducing the electronic resistivity of the SL-GDL-CF samples due to the formation of extra electron transport bridges in the carbon black matrix provided by the wire-like VGCFs interconnecting the disjoined carbon black particles. The cell performances of the PEMFCs fabricated with the as-prepared SL-GDL-CFs were likewise increased as VGCF loading increased both in the H_2/O_2 and H_2/air systems. In addition, the best performance obtained from the PEMFC fabricated with SL-GDL-CF15 was approximately 63% higher than that of the SL-GDL-CF0 in the H_2/O_2 system. Worth mentioning is that SL-GDL-CF15 is about 85% as efficient as ELAT GDL on the PEMFC performance for both the H_2/O_2 and H_2/air systems. The SL-GDL-CF samples, prepared with a simple and inexpensive process, are anticipated to have potential application in PEMFC.

Acknowledgements

The authors would like to thank Chung Yuan Christian University under grant CYCU-95-CR-CH and Yeu Ming Tai Chemical Industrial Co., Ltd., Taiwan (ROC) for their support to this research. Likewise, the authors extend their appreciation to Mr. J.J. Gong and Mr. S.M. Chang of the Materials and Electro-Optics Research Division, Elec-

tric Energy Section, Chung Shan Institute of Science and Technology for their evaluation of cell performance.

References

[1] Z. Qi, A. Kaufman, J. Power Sources 113 (2003) 37–43.
[2] G. Sasikumar, J.W. Ihm, H. Ryu, J. Power Sources 132 (2004) 11–17.
[3] G. Sasikumar, J.W. Ihm, H. Ryu, Electrochim. Acta 50 (2004) 601–605.
[4] J. Lee, J. Seo, K. Han, H. Kim, J. Power Sources 163 (2006) 349–356.
[5] H.L. Lin, T.L. Yu, K.S. Shen, L.N. Huang, J. Membr. Sci. 237 (2005) 1–7.
[6] L.R. Jordan, A.K. Shukla, T. Behrsing, N.R. Avery, B.C. Muddle, M. Forsyth, J. Appl. Electrochem. 30 (2000) 641–646.
[7] L.R. Jordan, A.K. Shukla, T. Behrsing, N.R. Avery, B.C. Muddle, M. Forsyth, J. Power Sources 86 (2000) 250–254.
[8] E. Passalacqua, G. Squadrito, F. Lufrano, A. Patti, L. Giorgi, J. Appl. Electrochem. 31 (2001) 449–454.
[9] M.V. Williams, E. Begg, L. Bonville, H.R. Kunz, J.M. Fenton, J. Electrochem. Soc. 151 (2004) A1173–A1180.
[10] S. Escribano, J.F. Blachot, J. Ethève, A. Morin, R. Mosdale, J. Power Sources 156 (2006) 8–13.
[11] M. Han, S.H. Chan, S.P. Jiang, J. Power Sources 159 (2006) 1005–1014.
[12] G.G. Park, Y.J. Sohn, S.D. Yim, T.H. Yang, Y.G. Yoon, W.Y. Lee, K. Eguchi, C.S. Kim, J. Power Sources 163 (2006) 113–118.
[13] H. Meng, C.Y. Wang, J. Electrochem. Soc. 151 (2004) A358–A367.
[14] B.R. Sivertsen, N. Djilali, J. Power Sources 141 (2005) 65–78.
[15] Y.W. Chen-Yang, T.F. Hung, J. Huang, F.L. Yang, J. Power Sources 173 (2007) 183–188.
[16] G.G. Tibbetts, Appl. Phys. Lett. 42 (1983) 666–668.
[17] M. Endo, Y.A. Kim, T. Hayashi, K. Nishimura, T. Matusita, K. Miyashita, M.S. Dresselhaus, Carbon 39 (2001) 1287–1297.
[18] M.S. Wu, J.T. Lee, P.C. Chiang, J.C. Lin, J. Mater. Sci. 42 (2007) 259–265.
[19] S.M. Sze, Physics of Semiconductor Device, second ed., John-Wiley & Sons, New York, 1981, pp. 30–32.
[20] V. Gurau, M.J. Bluemle, E.S. De Castro, Y.M. Tsou, J.A. Mann, T.A. Zawodzinski, J. Power Sources 160 (2006) 1156–1162.
[21] J. Comyn, Polymer Permeability, first ed., Elsevier Applied Science, New York, 1985, pp. 21–23.
[22] J. Moreira, A.L. Ocampo, P.J. Sebastian, M.A. Smit, M.D. Salazar, P. del Angel, J.A. Montoya, R. Pérez, L. Martínez, Int. J. Hydrogen Energy 28 (2003) 625–627.
[23] M. Kim, J.N. Park, H. Kim, S. Song, W.H. Lee, J. Power Sources 163 (2006) 93–97.
[24] F. Lufrano, E. Passalacqua, G. Squadrito, A. Patti, L. Giorgi, J. Appl. Electrochem. 29 (1999) 445–448.